



Article

Monodisperse MoS₂/Graphite Composite Anode Materials for Advanced Lithium Ion Batteries

Baosheng Liu *, Feng Li, Hongda Li , Shaohui Zhang, Jinghua Liu, Xiong He, Zijun Sun, Zhiqiang Yu , Yujin Zhang, Xiaoqi Huang, Fei Guo, Guofu Wang and Xiaobo Jia

School of Electronic Engineering, Guangxi University of Science and Technology, No. 2 Wen-Chang Road, Liuzhou 545006, China

* Correspondence: liubaosheng@gxust.edu.cn

Abstract: Traditional graphite anode material typically shows a low theoretical capacity and easy lithium decomposition. Molybdenum disulfide is one of the promising anode materials for advanced lithium-ion batteries, which possess low cost, unique two-dimensional layered structure, and high theoretical capacity. However, the low reversible capacity and the cycling-capacity retention rate induced by its poor conductivity and volume expansion during cycling blocks further application. In this paper, a collaborative control strategy of monodisperse MoS₂/graphite composites was utilized and studied in detail. MoS₂/graphite nanocomposites with different ratios (MoS₂:graphite = 20%:80%, 40%:60%, 60%:40%, and 80%:20%) were prepared by mechanical ball-milling and low-temperature annealing. The graphite sheets were uniformly dispersed between the MoS₂ sheets by the ball-milling process, which effectively reduced the agglomeration of MoS₂ and simultaneously improved the electrical conductivity of the composite. It was found that the capacity of MoS₂/graphite composites kept increasing along with the increasing percentage of MoS₂ and possessed the highest initial discharge capacity (832.70 mAh/g) when MoS₂:graphite = 80%:20%. This facile strategy is easy to implement, is low-cost, and is cosmically produced, which is suitable for the development and manufacture of advanced lithium-ion batteries.

Keywords: lithium-ion battery anode; molybdenum disulfide; graphite; mechanical ball-milling; composite materials



Citation: Liu, B.; Li, F.; Li, H.; Zhang, S.; Liu, J.; He, X.; Sun, Z.; Yu, Z.; Zhang, Y.; Huang, X.; et al.

Monodisperse MoS₂/Graphite Composite Anode Materials for Advanced Lithium Ion Batteries. *Molecules* **2023**, *28*, 2775. <https://doi.org/10.3390/molecules28062775>

Academic Editor: Federico Bella

Received: 24 February 2023

Revised: 14 March 2023

Accepted: 17 March 2023

Published: 19 March 2023



Copyright: © 2023 by the authors. Licensee MDPI, Basel, Switzerland. This article is an open access article distributed under the terms and conditions of the Creative Commons Attribution (CC BY) license (<https://creativecommons.org/licenses/by/4.0/>).

1. Introduction

Energy is an important foundation to support the continuous development of human society. Energy scarcity, the breeding of environmental pollution, and other problems have aroused widespread concern in today's era of high energy and high consumption, as well as rapid technological development. The large-scale use of traditional non-renewable energy sources is bound to cause environmental problems such as the ozone hole and the greenhouse effect, which seriously threaten human health [1]. In this context, lithium-ion batteries have rapidly developed into a new generation of energy-storage power supplies based on their characteristics of high specific capacity, high cycle life, small size, light weight, no memory effect, and no pollution. The traditional graphite anode material has a low theoretical capacity (theoretical capacity of 372 mAh/g [2–4]), and it is easy to form lithium dendrites at room temperature and low temperature, resulting in poor cyclic stability, reduced safety, and other problems that can no longer meet the demand for the high energy density and high power density of power batteries [5–7].

To solve the above problems, some researchers have focused on two-dimensional materials with unique structures [8–10], among which molybdenum disulfide is favored by researchers due to its high theoretical specific capacity (670 mAh/g), low cost, and layered structure that facilitates Li⁺ de-embedding [11]. Considering that MoS₂ has poor electrical conductivity and is prone to agglomeration during charging and discharging,

resulting in poor cycling stability, the widely adopted solution is to combine MoS₂ with materials of strong electrical conductivity and stabilization, which has a synergistic effect and then improves the electrochemical properties, such as cycling stability. In the research work of Ma et al. [12], hierarchical carbon/MoS₂ composites were successfully prepared via the facile hydrothermal method to enhance the electrochemical performance of MoS₂ anodes for lithium-ion batteries. The porous structure could provide a rapid transport path for lithium-ion diffusion, which effectively improved the cycling stability of the anode material. However, the presence of porous carbon does not effectively improve the discharge capacity of the composite, which is what needs to be addressed. Hai et al. [13] prepared MoS₂/carbon nanotube composites by a high-energy mechanical grinding method and found that the discharge-specific capacity and cycling capacity retention of the materials were significantly improved when the mass ratio of molybdenum disulfide to carbon nanotubes was 1:2, the first discharge capacity was as high as 1703 mAh/g at a current density of 100 mA/g, and the capacity retention was around 85% after 70 cycles. The introduction of MoS₂ effectively improves the discharge capacity, and carbon nanotubes can act as a bridge between the layers of molybdenum disulfide, solving the drawback that lithium ions cannot be efficiently transported between the composite layers. The problem in this work is that multi-walled carbon nanotubes are expensive and cannot meet the requirements of low cost and high yield in the production of anode materials for lithium-ion batteries. Considering the inherent structural collapse of molybdenum disulfide during cyclic charge/discharge, many researchers have optimized the structure of molybdenum disulfide during its preparation to improve its electrochemical properties. Qi et al. [14] successfully synthesized molybdenum disulfide/reduced graphene oxide (MoS₂/rGO) composites by the hydrothermal method. The rGO interconnections provide excellent conductive networks for the lamellar structure and can act as a carrier for the growth of molybdenum disulfide nanosheets to achieve structural support. But this work may produce atomic-scale defects in the substrate when preparing graphene oxide dispersion by the Hummer method, which will have an impact on the morphology of the composites [15].

Among many material compounding processes, carbon cladding modification is a very common means of surface modification that can significantly improve the electrical conductivity of the material. Jin et al. [16] prepared a carbon-coated molybdenum disulfide (C@MoS₂) composite material for lithium-ion battery anode material by the hydrothermal in situ method. Studies have shown that the composite material has a porous carbon-coated structure and good electrochemical performance. After 200 cycles at the current density of 500 mA/g, the capacity retention rate is as high as 94%. But the current carbon cladding process and the preparation process of advanced carbon materials are relatively complex, and the production cost of electrode materials prepared on this basis is high, which is still not conducive to commercial application. In addition to the above methods, nano-sizing MoS₂ materials is also an effective way to improve their cycling performance, but nanoparticles are characterized by both low first-cycle Coulomb efficiencies and complicated preparation processes. Therefore, the research on the technology of micro and nano composite structures (microscale particles with built-in nanoscale features) of materials will be very promising after satisfying the conditions of commercial feasibility such as safety and cost [17].

In comparison to the previous research, compounding the most widely used graphite anode material in the industry with two-dimensional molybdenum disulfide materials, while providing sufficient electrical conductivity and depolarization, is conducive to a reduced technology route in the battery industry to achieve graphite anode replacement at a lower cost [18]. Based on this idea, in this paper, MoS₂/graphite composites were prepared from monodisperse nano-layered molybdenum disulfide [19] and conventional graphite anode materials by mechanical ball-milling, and the ball-milling process resulted in a uniform distribution of graphite sheets between MoS₂ sheets, which both slowed down the agglomeration of MoS₂ and improved the electrical conductivity of the composites, showing excellent electrochemical properties overall. This method provides new ideas

for the design and optimal modification of high-performance lithium-ion battery cathode materials, which can effectively contribute to the rapid development of new energy vehicle power battery technology research.

2. Results and Discussion

2.1. Structure and Morphology of MoS₂/Graphite Composites with Different Ratios

The X-ray diffractograms of the anode materials with different composite ratios of MoS₂/graphite are shown in Figure 1a, and it can be seen that all four composite anode materials show a crystal structure similar to the intrinsic MoS₂; the diffraction peaks shown in the figure (14.4° (002), 32.7° (100), 39.3° (103), 49.8° (105), and 58.3° (110)) all correspond to the diffraction peaks of the hexagonal crystal structure of molybdenum disulfide [20]; and the peaks appear in perfect agreement when compared with the standard card PDF # 37-1492. Moreover, the peak positions and peak shapes of all diffraction peaks are clear, indicating that the composite anode material has high crystallinity and purity. In addition, a diffraction peak of varying intensity was observed at 26.5° in the diffractograms of the four MoS₂/graphite composites with different ratios, which proved the presence of graphite and coincided with the expected results that the intensity of this peak was decreasing as the percentage of graphite material in the composites decreased. In contrast, the intensity of the MoS₂ characteristic peak does not increase as its percentage increases, because the change in the intensity of the MoS₂ characteristic peak reflects the change in the number of layers of the two-dimensional material, which indicates that the number of layers of the MoS₂ material does not change after ball-milling [21]. No other obvious spurious peaks were detected, indicating that no impurities were generated and the original structure of the composite was not destroyed during the ball-milling process. In addition, it can be seen in Figure 1b that the characteristic peak of the MoS₂ material at 14.6° (2θ) has significantly shifted to the left after ball-milling, which further indicates that the ball-milling process may have made the crystallite size of the MoS₂ material larger. In contrast, the characteristic peak at 26.6° (2θ) of the graphite material after ball-milling has slightly shifted to the right, which indicates that the ball-milling process has no significant effect on the crystallite size of the graphite material.

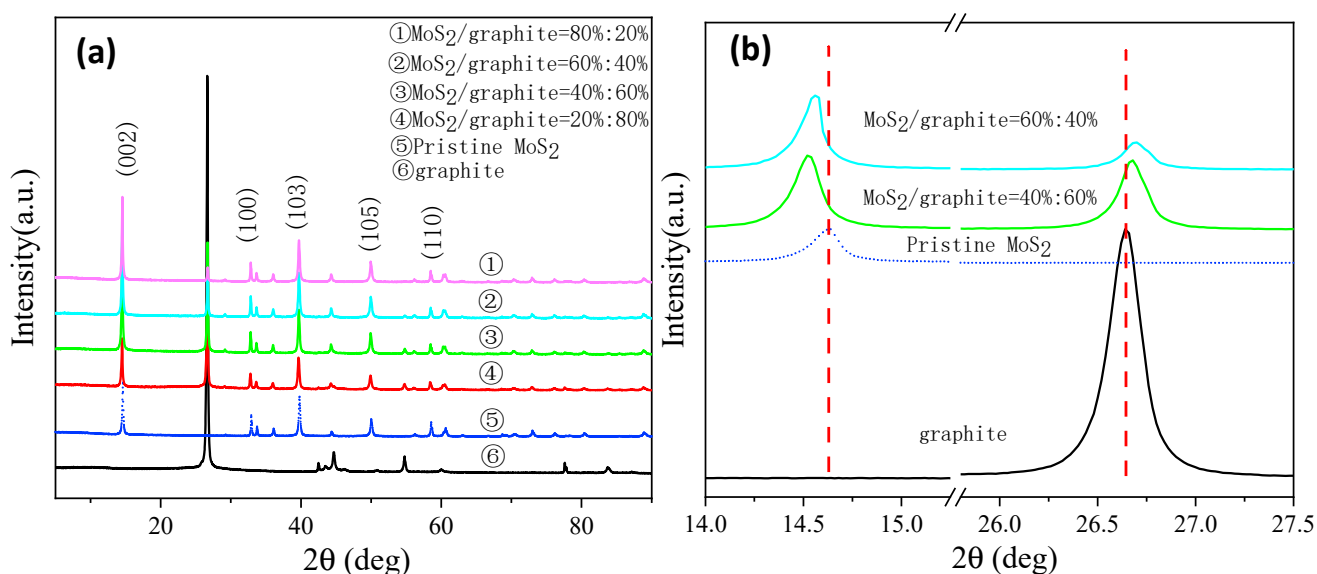


Figure 1. (a) XRD patterns of MoS₂/graphite composites at different proportions; (b) Partial XRD patterns.

The SEM images of graphite, intrinsic MoS₂ and MoS₂/graphite composite anode materials are shown in Figure 2. The morphology of the intrinsic graphite material is a flattened sphere with a particle size of 9 μm (Figure 2a), and the morphology of the intrinsic molybdenum disulfide material is a monodisperse nanolayer (Figure 2b), which has the

advantages of uniform particle size, high activity, a large specific-surface area, and a high sample-adsorption capacity [22,23]. By comparison, the morphology of the MoS_2 /graphite composites was found to be significantly different from that of the intrinsic graphite material (Figure 2a) and the intrinsic molybdenum disulfide material (Figure 2b) [24]. The graphite in its original flattened spherical form is dispersed into thin flake layers by a ball-milling process [25], and the molybdenum disulfide is simultaneously ball-milled into flake structures. The lamellar graphite effectively enters between the MoS_2 flakes and mixes uniformly to form compacted aggregates. By comparing Figure 2c–f, it can be found that with the increasing percentage of MoS_2 , it can be observed that the lumpy particles are reduced and MoS_2 is uniformly dispersed. When the particle size of the graphite material is significantly reduced and the percentage of molybdenum disulfide reaches 80%, the particle size of the composite is mostly between 1–2 μm . By observation, Figure 2f shows mostly flaky MoS_2 material, whose discharge capacity is expected to be enhanced by a large amount of molybdenum disulfide. Overall, the compounded MoS_2 /graphite aggregates can effectively increase the contact area between the material and electrolyte, alleviate the agglomeration phenomenon, and improve the discharge capacity, but the excessive MoS_2 will reduce the cycling stability.

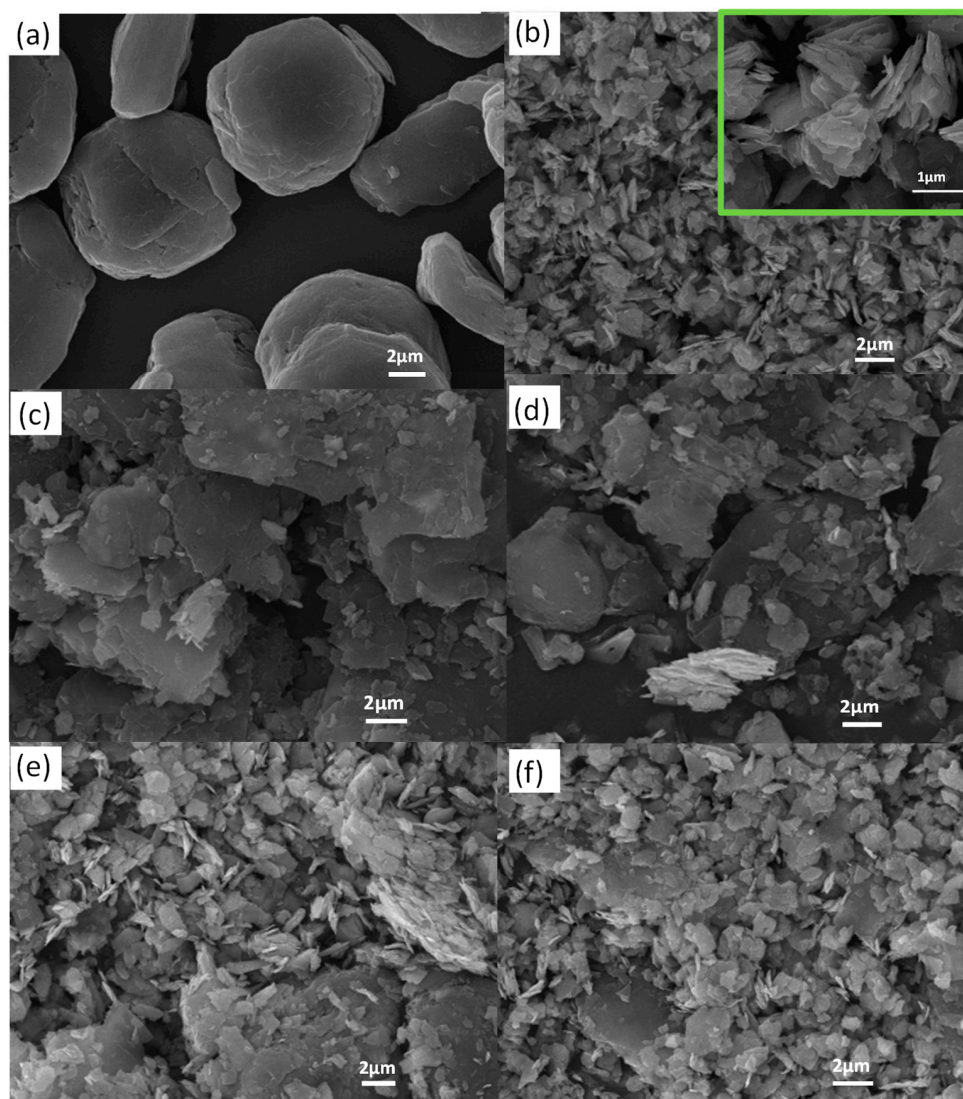


Figure 2. SEM images: (a) Graphite; (b) MoS_2 (The image obtained after zooming in is shown in the green box); (c) MoS_2 /graphite (20%:80%); (d) MoS_2 /graphite (40%:60%); (e) MoS_2 /graphite (60%:40%); (f) MoS_2 /graphite (80%:20%).

To further characterize the dispersion of MoS₂ material in MoS₂/graphite composites, EDS tests were conducted on four MoS₂/graphite composites with different ratios, and the test results are shown in Figure 3. It is easy to see that with the increasing percentage of MoS₂, the Mo elements and S elements in the composites become more and more obvious, and in addition, it is obvious through the four graphs in Figure 3 that the elements such as Mo, S, and C in the composites are uniformly distributed without any abnormal phenomena such as agglomeration, which indicates that the MoS₂ materials are very uniformly compounded with graphite materials and play a positive role in improving the electrochemical performance of the anode materials [26].

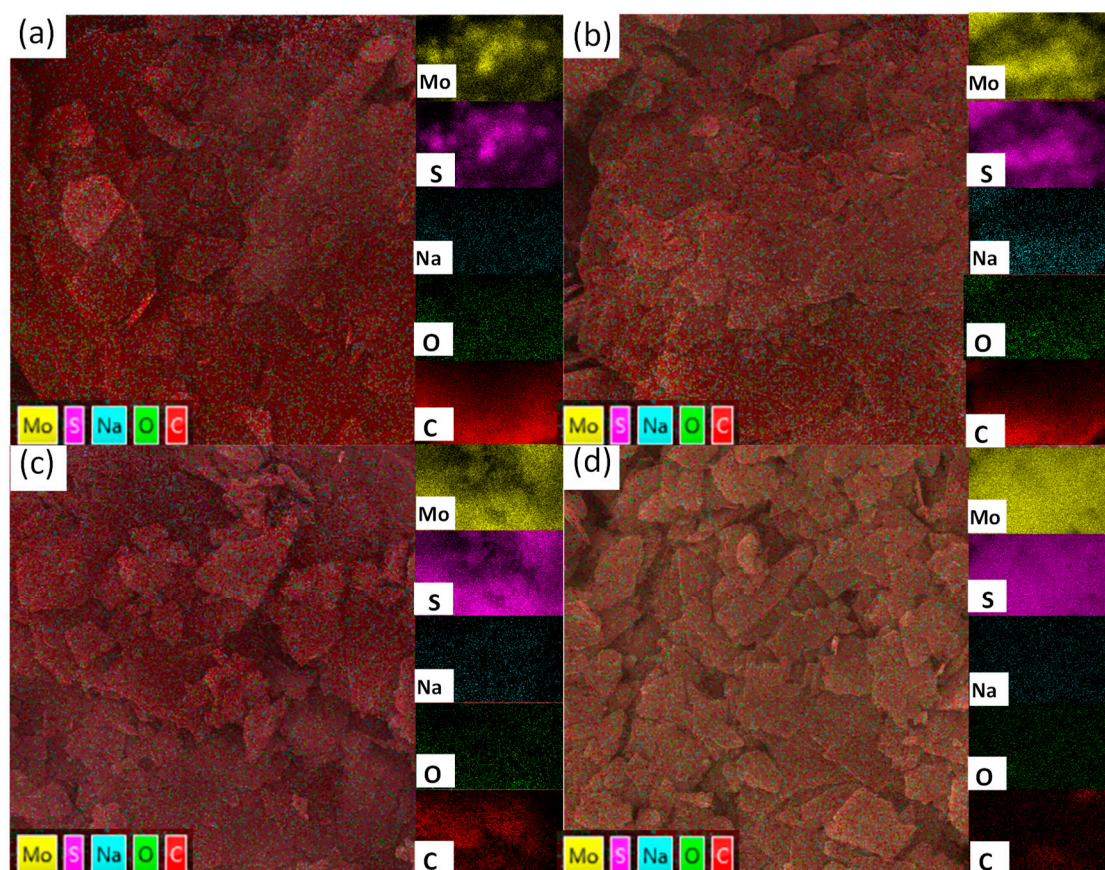


Figure 3. EDS images: (a) MoS₂/graphite (20%:80%); (b) MoS₂/graphite (40%:60%); (c) MoS₂/graphite (60%:40%); (d) MoS₂/graphite (80%:20%).

2.2. Electrochemical Properties of MoS₂/Graphite Composites with Different Proportions

Initial charge–discharge curves, various current–capacity tests, and cycling tests (0.05 C/1 C) were conducted on the prepared coin-cell in the voltage range of 0.05–3.00 V to study the electrochemical performance of MoS₂/graphite anode materials with different composite ratios. The test results with the contrast of graphite anode are shown in Figure 4.

Figure 4a shows the activation performance of the MoS₂/graphite composite anode materials under the same test conditions, and the first discharge capacities of the MoS₂/graphite (20%:80%, 40%:60%, 60%:40%, and 80%:20%) composites were 542.127 mAh/g, 615.768 mAh/g, 787.463 mAh/g, and 832.699 mAh/g, respectively. The first discharge capacity of MoS₂/graphite composite increases as the percentage of molybdenum disulfide increases, with the highest discharge capacity, achieved when the percentage of molybdenum disulfide was 80%, which is approximately twice that of the intrinsic graphite material. Therefore, it can be concluded that the increase in the capacity of MoS₂/graphite composites is attributed to the presence of elemental sulfur in molybdenum disulfide [27]. Graphite plays an important role in making up the difference in the conductivity of molybdenum

disulfide in composites. The first Coulomb efficiencies of the MoS₂/graphite (20%:80%, 40%:60%, 60%:40%, and 80%:20%) composites with different ratios were 97.50%, 93.84%, 86.23%, and 87.84%, showing a decreasing trend due to the higher percentage of molybdenum disulfide in the composite; the more obvious is its volume expansion and structural collapse [28].

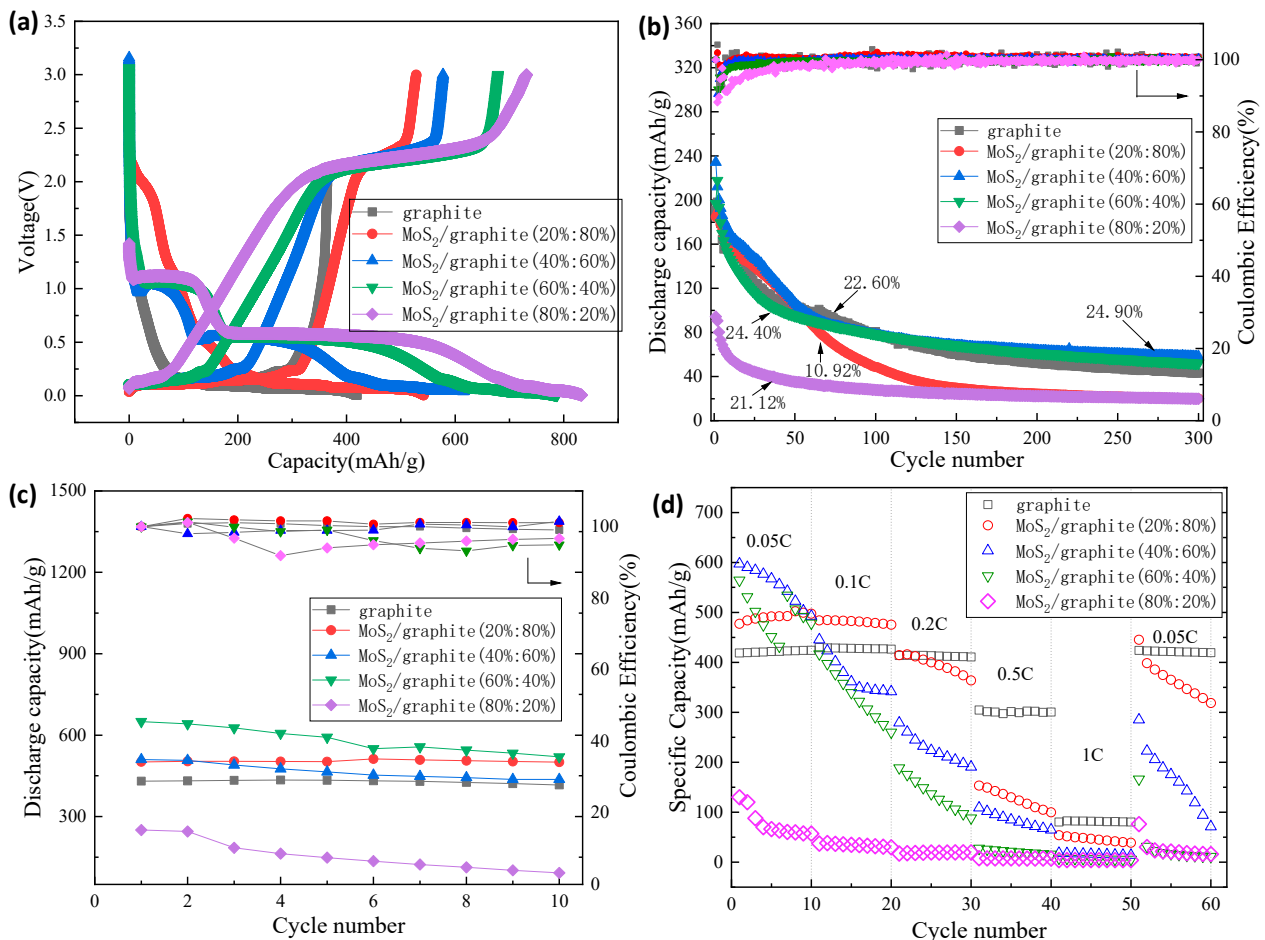


Figure 4. (a) Initial charge–discharge capacity curve; (b) 1 C cycling; (c) 0.05 C cycling; (d) Rate capability curve.

Cycle performance is an important indicator to measure the electrochemical performance of lithium-ion batteries [29]. Figure 4b shows that MoS₂:graphite = 20%:80% and MoS₂:graphite = 40%:60%, MoS₂:graphite = 60%:40%, MoS₂:graphite = 80%:20% in the voltage range of 0.05–3.00 V, the performance curve of 300 cycles of constant current charge/discharge under the condition of 1 C high rate. The results show that, with the increase in the proportion of MoS₂, the cycle performance of the composite material shows a trend of first increasing and then decreasing. After 300 cycles, when MoS₂:graphite = 40%:60%, the cycle-capacity retention rate is the best, and the cycle capacity is the highest at 58.328 mAh/g with 99.89% coulombic efficiency, showing that this composite ratio of electrodes has excellent reversibility. When MoS₂:graphite = 80%:20%, the initial capacity of the composite material is the lowest at 19.936 mAh/g, and the cycle capacity retention rate is also the worst (only 21.12%), which is far lower than the discharge capacity of the intrinsic graphite anode material. The reason is that when charging and discharging under high-rate conditions, due to the excessive proportion of molybdenum disulfide in the MoS₂/graphite composite material, the structure of the composite material is destroyed along with the intercalation and deintercalation of Li⁺ [30].

Figure 4c depicts the performance curves of the four composite materials under constant current charge and discharge conditions at 0.05 C. It can be concluded that the cycle capacity retention rate of MoS₂/graphite (20%:80%, 40%:60%, 60%:40%, and 80%:20%) composites shows a downward trend with the increase of the proportion of MoS₂ (99.80%, 85.67%, 79.97%, and 36.83%), and when MoS₂:graphite = 80%:20%, the capacity of the composite material is already much lower than that of the intrinsic graphite anode material. When MoS₂:graphite = 20%:80%, the discharge-specific capacity does not seem to change after cycling, and the cycle-capacity retention rate is as high as 99.80%, with 99.93% coulombic efficiency, which shows that a large number of graphite sheets are evenly distributed between the molybdenum disulfide sheets, which stabilizes the MoS₂/graphite composite structure and enabling the electrode to obtain excellent reversibility. When MoS₂:graphite = 80%:20%, the cycle performance is the worst, and the capacity retention rate is only 36.83%. Along with the decreasing percentage of C elements in MoS₂/graphite materials, the electrical conductivity and structural stability of the composites will continue to deteriorate, which is the reason for the decreasing trend of the cyclic capacity retention of the composites [31].

For the practical application of lithium batteries, electrodes must have excellent reversible rate performance. The rate capability of both graphite and MoS₂/graphite electrodes was measured, ranging from low to high charge/discharge rates, i.e., 0.05, 0.1, 0.2, 0.5, and 1 C (Rated current capacity, and 1C charging or discharging means that the battery is fully charged or fully discharged within 1 h.), as illustrated in Figure 4d. It can be found that when the charge and discharge test is performed under low-rate conditions, the composite material with a small proportion of molybdenum disulfide has a higher discharge capacity. When the charge/discharge rate increases, the MoS₂/graphite composite material shows poor stability, and its cycling capacity also shows a downward trend, which shows that the MoS₂/graphite composite material has poor adaptability to the change of charge/discharge current. The reason for this problem is inseparable from the characteristics of the molybdenum disulfide material itself, such as poor conductivity and an unstable structure during cycling. Solving this problem will be our next research project.

In order to explore the reasons for the decrease in the specific capacity of the graphite electrode and MoS₂/graphite composite electrode, SEM tests were conducted on the pole pieces before and after 300 cycles at 1 C rate, and the test results are shown in Figure 5. We further analyzed that the graphite electrode flakes exhibit the morphological characteristics that the conductive agent uniformly adheres to the graphite material surface before cycling and the contact between them is excellent (Figure 5a); the MoS₂/graphite composite electrode flakes exhibit a clear two-dimensional lamellar monodisperse structure, and this structure also allows the close contact between the active material and the conductive agent (Figure 5b) [32]. The decrease in the specific capacity of graphite electrode sheet after cycling can be attributed to the formation of a thick and rough SEI layer covering the surface of electrode material by the side reaction with electrolyte (Figure 5c) [33,34]; meanwhile, along with the cyclic charging and discharging, more obvious cracks appear on the surface of graphite electrode (Figure 5e), which will be very unfavorable to the contact between the active material and conductive agent [35]. For the MoS₂/graphite composite electrode, the irreversibly grown SEI layer that forms is thinner and more stable (Figure 5d), but the formation process also consumes a large amount of electrolyte, which leads to the electrolyte drying phenomenon and further decreases the specific capacity of the MoS₂/graphite composite electrode [36,37]. In addition, some cracks were also observed on the surface of the MoS₂/graphite composite electrode after cycling (Figure 5f), and these cracks would deteriorate the contact between the active substance and the conducting agent, thus causing a sharp decrease in the specific capacity of the MoS₂/graphite composite electrode.

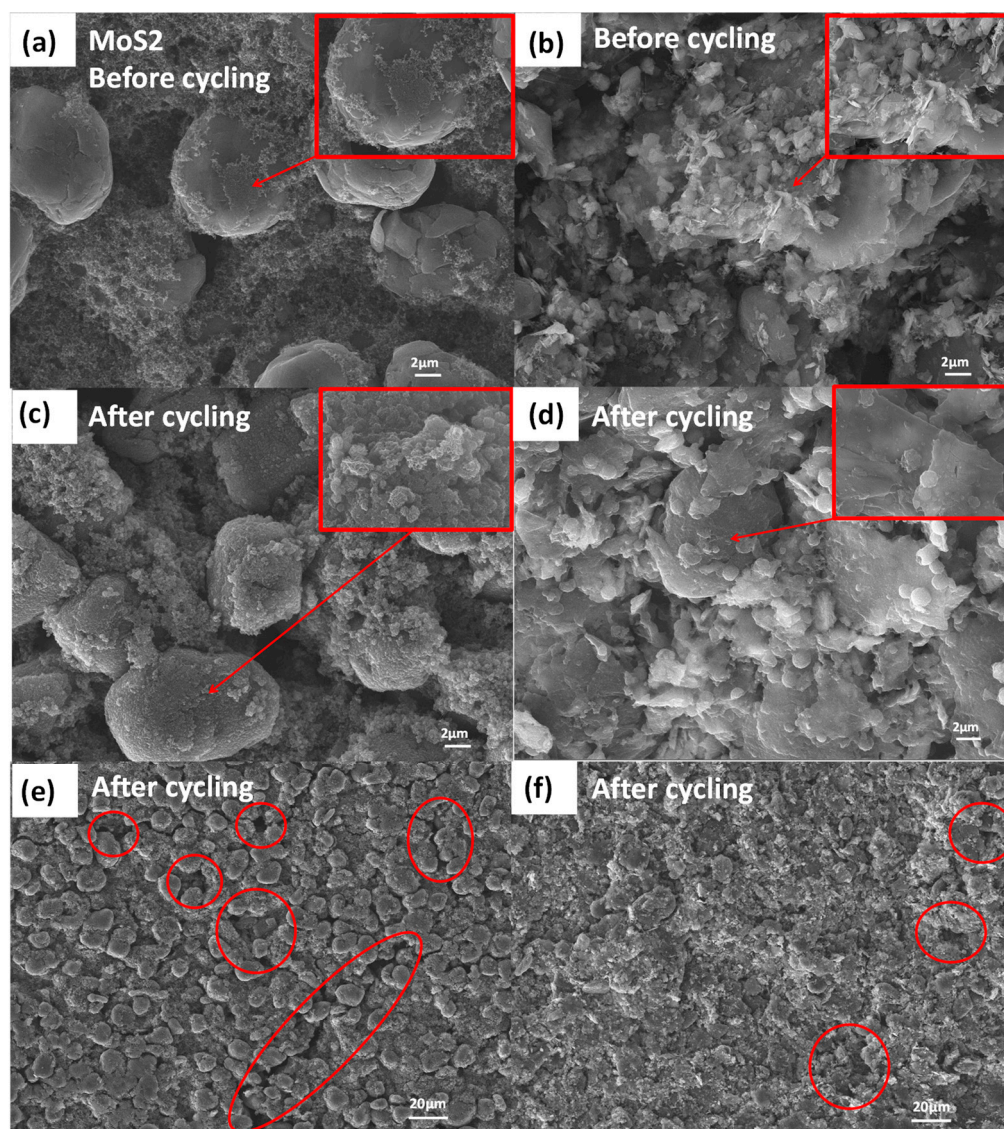
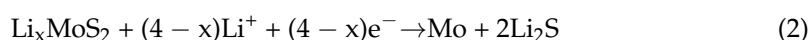
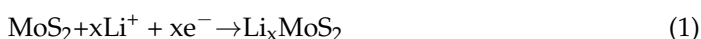


Figure 5. SEM image of the electrode before and after 300 cycles at 1C rate: (a) Graphite electrode before cycling; (b) MoS₂/graphite electrode before cycling; (c,e) Graphite electrode after cycling; (d,f) MoS₂/graphite electrode after cycling.

Figure 6a shows the cyclic voltammetry test curves of intrinsic graphite materials and MoS₂/graphite composites with four different ratios in the voltage range of 0.05–3.00 V. For the first cathodic process, the MoS₂/graphite electrode depicts cathodic peaks between 0.75–1.25 V and 1.50–2.00 V. The reduction peaks between 1.50 and 2.00 V can be attributed to the intercalation of Li⁺ into the layered structure of MoS₂ to form Li_xMoS₂. The peak between 0.75 and 1.25 V is attributed to the conversion of Li_xMoS₂ [38] into metallic Mo and Li₂S, respectively. The reaction process is shown in reaction Equation (1) and reaction Equation (2) [39].



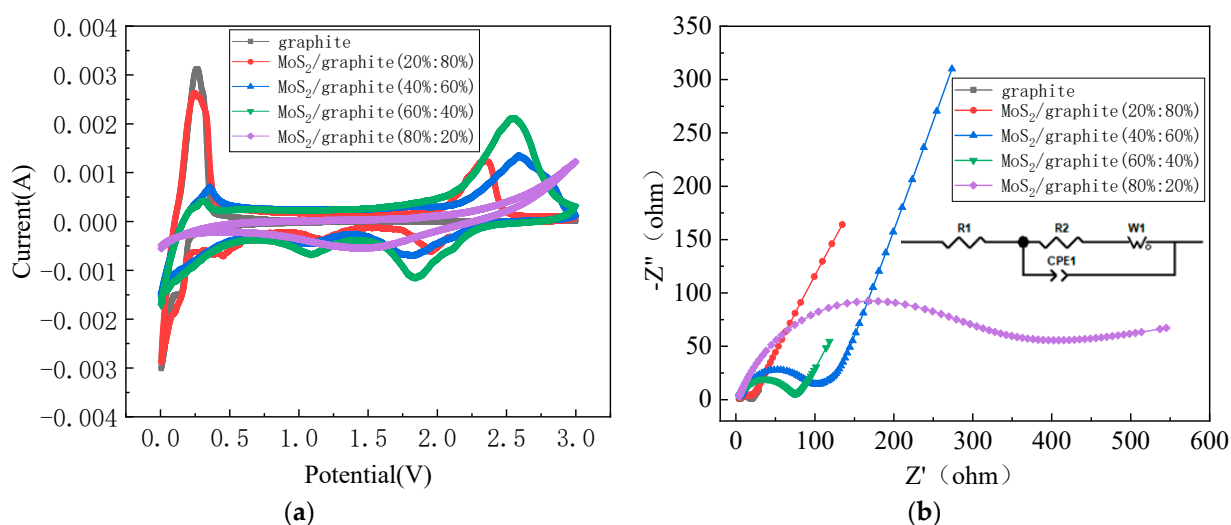


Figure 6. (a) CV test curves; (b) EIS test curves.

In the reverse anodic process, the MoS₂/graphite composite material has an obvious oxidation peak in the voltage range of 2.25–3.00 V, which may be related to the oxidation of Li₂S to S; the reaction process is shown in reaction Equation (3). In addition, a series of redox peak pairs between 0.05 and 0.27 V is related to the intercalation and exportation of Li⁺ on graphite interlayer carbon atoms.

The electrochemical impedance spectra (EIS) of graphite and MoS₂/graphite are shown in Figure 6b. The intercept of the curve at high frequency with the axis corresponds to electrolyte resistance and contact resistance. The inset of Figure 6b is the equivalent circuit of an EIS fitting; R₁ is the ohmic resistance of the electrode, and R₂ is the charge transfer resistance. CPE1 is an abbreviation for the constant phase elements. W₁ is the Warburg impedance [40]. The R₁ value of the graphite and MoS₂:graphite = 20%:80%, 40%:60%, 60%:40%, and 80%:20% electrodes is calculated to be 4.73 Ω, 4.09 Ω, 5.39 Ω, 3.84 Ω, and 4.16 Ω, respectively, indicating that the ohmic resistance of the above electrodes in this study were very close and the errors in the preparation process were relatively small. According to the inserted equivalent circuit [41], the R₂ value of the graphite and MoS₂:graphite = 20%:80%, 40%:60%, 60%:40%, and 80%:20% electrodes is calculated to be 19.57 Ω, 16.04 Ω, 106.89 Ω, 74.97 Ω, and 428.64 Ω. When MoS₂:graphite = 20%:80%, the charge-transfer impedance is the smallest, and its slope in the low-frequency region is the largest, indicating that the diffusion resistance of Li⁺ in the electrode at this time is the smallest. It can be concluded that an appropriate amount of MoS₂ combined with a graphite material with better conductivity can have a synergistic effect to reduce the charge transfer resistance of the composite material and improve the diffusion efficiency of Li⁺ [42].

3. Experiment

3.1. Preparation of Anode Materials

In this experiment, 0.45 g of sodium molybdate dihydrate (Na₂MoO₄·2H₂O, Aladdin Reagent Co., Shanghai, China) and 0.6 g of thiourea (CH₄N₂S, Aladdin Reagent Co., Shanghai, China) were first mixed in 36 mL of deionized water (Molecular Lab water ultra-purifier, Shanghai, China) as precursors, and the well-mixed solution was transferred into a 100 mL Teflon-lined stainless steel autoclave (Hefei kejing materials technology Co., Ltd., Hefei, China) and sealed tightly, and heated at 220 °C for 24 h in a furnace [43,44]. After cooling naturally, the black precipitates were collected by centrifugation, washed with deionized water and anhydrous ethanol (C₂H₅OH, Sinopharm Chemical Reagent Co., Shanghai, China), and dried in a vacuum oven at 80 °C for 24 h [45,46]. The as-prepared MoS₂ was annealed in a conventional tube furnace at 500 °C for 2 h in a stream

of argon gas (Ar, Liuzhou Xineng Gas Co., Liuzhou, China) [47]. Finally, monodisperse nano-layered molybdenum disulfide was obtained. The graphite anode material was selected from the 918 series of natural graphite (C, Tianjin Battery Co., Tianjin, China) with excellent cycling performance and multiplicative performance [48,49]. The prepared molybdenum disulfide powder and natural graphite were mixed in four different ratios of MoS₂:graphite = 20%:80%, 40%:60%, 60%:40%, and 80%:20% to investigate the effect of different MoS₂ contents on the anode performance. The four ratios of anode materials were put into four agate ball-milling jars, and anhydrous ethanol was poured in to avoid oxidation of the anode materials during the ball-milling process until the anhydrous ethanol covered the agate balls in the ball-milling jars [50,51]. The four different proportions of composite materials were ball-milled at low speed at 50 Hz for 2 h to fully mix them, then placed in a blast drying oven at 60 °C for 24 h. After all the anhydrous ethanol evaporated, the composite powder was collected.

3.2. Preparation of Button Cell

The 0.8 g of MoS₂/graphite composite anode material, 0.1 g of super P (Sinopharm Chemical Reagent Co., Shanghai, China), and 0.1 g of CMC (Carboxymethyl Cellulose Sodium, Shanghai Macklin Biochemical Co., Shanghai, China) were poured into the weighing bottle according to the mass ratio of 8:1:1, and the appropriate amount of deionized water and N-Methylpyrrolidone (NMP, Shanghai Aladdin Biochemical Co., Shanghai, China) was added according to the fluidity state of the material for stirring [52], and then it was stirred into a slurry with good fluidity and evenly coated on the matte surface of the clean copper foil (Hefei kejing materials technology Co., Ltd.), and then it was put into a vacuum oven and dried at 120 °C for 8 h [53]. After rolling, copper foil coated with anode material was cut into 12 mm-diameter round anode sheets by a cutting machine, and then the round anode sheet was weighed (the mass of the active material used in the electrode sheet was about 11 mg). After weighing, the anode sheet was placed in a paper package and placed in a vacuum-drying oven for 8 h at 120 °C. The average areal mass loading of the active materials was around 2.43 mg/cm². To ensure the influence of the environment on the preparation process of anode material, the anode material preparation process should be carried out in an environment with a humidity of 20% or less.

The standard button cells (CR2025) were assembled in an argon-filled glovebox (O₂ ≤ 0.01 ppm and H₂O ≤ 0.01 ppm), using MoS₂/graphite electrodes as working electrodes and lithium metal chips (0.45 × 15.6 mm, Neware Technology Ltd., Shenzhen, China) as the counter electrode. Two insulating separators (2400 Celgard PP membrane) were used to prevent short-circuiting of the cell. The electrolyte (Jiangxi Jinhui Lithium Electric Materials Co., Ltd., Jiangxi, China) was composed of 1 M LiPF₆ in ethylene carbonate (EC), diethyl carbonate (DEC), and ethyl methyl carbonate (EMC) mixed solution (EC: DEC: EMC = 1:1:1 vol%) [54].

3.3. Material Structure and Morphology Characterization Testing

The crystal atomic structure of the sample to be tested was determined by an XRD (X-ray diffraction) test, and the phase composition of the material was analyzed qualitatively and quantitatively. The test instrument was Rigaku SmartLab SE, Japan. The test range was 5–90°, the scan rate was 5°/min, and the light source was Cu-Kα ray. The tube voltage was 40 kV, the tube current was 40 mA, and the scanning mode was continuous scanning. The TESCAN MIRA LMS (Czech Republic) was used for scanning electron microscopy (SEM) testing to observe the surface morphology, smoothness, and particle size of the cathode material at the microscopic level. Qualitative and quantitative analysis of elements can be performed by analyzing the types and compositions of elements with energy-dispersive X-ray spectroscopy (EDS).

3.4. Electrochemical Performance Testing

The previously assembled button cell in the glove box was transferred into the thermostat (thermostat temperature was 25 °C), and the constant current charge/discharge performance test was conducted in the test voltage range of 0.05–3.00 V (the test instrument was selected from Shenzhen Xinwei Battery Testing System BTS4000). AC impedance test (EIS) and cyclic voltammeter test (CV) needed to be tested on the electrochemical workstation (model CHI760E), with a test voltage range of 0.05–3.00 V, AC impedance spectrum test set frequency range of 0.01–100 000 Hz, the amplitude of 5 mV, bias current below 0.01 Hz, using Fourier transform. The scanning speed of the cyclic voltammeter test was 0.1 mV/s.

4. Conclusions

In this study, the outstanding electrochemical performance of MoS₂/graphite composites could be attributed to the following reasons: After ball-milling, the MoS₂ sheets and graphite sheets are uniformly dispersed. The presence of molybdenum disulfide enhances the overall capacity, and the graphite sheets effectively alleviate the agglomeration of MoS₂ and improve electrical conductivity. As evidenced by characterization testing, the MoS₂/graphite composite anode material has high crystallinity and purity. The electrochemical performance test shows that the capacity of MoS₂/graphite composites possessing the highest first discharge capacity occurred when MoS₂:graphite = 80%:20%; after 300 cycles of charge/discharge at high magnification (1 C), it was found that the highest reversible capacity occurred when MoS₂:graphite = 40%:60%; the cyclic charge/discharge test results at a low rate (0.05 C) showed that the MoS₂/graphite composites showed the best cycling performance when MoS₂:graphite = 20%:80%. To sum up, different composite proportions can improve the different electrochemical performances of the battery. The performance research and analysis of four different proportions of MoS₂/graphite composite materials in this paper demonstrate a promoting and guiding role in the further optimization and development of high-performance lithium-ion battery anode materials.

Author Contributions: Writing—original draft preparation, B.L.; writing—review and editing, B.L., F.L., H.L., S.Z., J.L., X.H. (Xiong He), Z.S., Z.Y., Y.Z., X.H. (Xiaoqi Huang), F.G., G.W. and X.J.; conceptualization, B.L.; methodology, F.L.; validation, Y.Z. and X.H. (Xiaoqi Huang); data curation, B.L. and F.L.; supervision, B.L. and H.L.; funding acquisition, B.L. All authors have read and agreed to the published version of the manuscript.

Funding: Doctoral Foundation of Guangxi University of Science and Technology (Grant No. 18Z13). Shandong Province Science and Technology Small and Medium-sized Enterprises Innovation Ability Improvement Project (Grant No. 2022TSGC2519). Guangxi Scientific Base & Talent Special Project (AD20297084).

Institutional Review Board Statement: Not applicable.

Informed Consent Statement: Not applicable.

Data Availability Statement: The data presented in this study are available on request from the corresponding author.

Conflicts of Interest: The authors declare no conflict of interest.

Sample Availability: Samples of graphite and molybdenum disulfide are available from the author.

References

1. Rojaee, R.; Shahbazian-Yassar, R. Two-Dimensional Materials to Address the Lithium Battery Challenges. *ACS Nano* **2020**, *14*, 2628–2658. [[CrossRef](#)]
2. Cha, E.; Kim, D.K.; Choi, W. Advances of 2D MoS₂ for High-Energy Lithium Metal Batteries. *Front. Energy Res.* **2021**, *9*, 645403. [[CrossRef](#)]
3. Wenelska, K.; Adam, V.; Thauer, E.; Singer, L.; Klingeler, R.; Chen, X.; Mijowska, E. Fabrication of 3D graphene/MoS₂ spherical heterostructure as anode material in Li-ion battery. *Front. Energy Res.* **2022**, *10*, 960786. [[CrossRef](#)]

4. Wu, J.; Ciucci, F.; Kim, J.-K. Molybdenum Disulfide Based Nanomaterials for Rechargeable Batteries. *Chem.-A Eur. J.* **2020**, *26*, 6296–6319. [[CrossRef](#)] [[PubMed](#)]
5. Zhang, D.; Zhang, C.; Lu, F.; Jiang, H.; Wei, F. Si-induced insertion of Li into SiC to form Li-rich SiC twin crystal. *Particuology* **2023**, *74*, 56–63. [[CrossRef](#)]
6. Qian, H.; Ren, H.; Zhang, Y.; He, X.; Li, W.; Wang, J.; Hu, J.; Yang, H.; Sari, H.M.K.; Chen, Y.; et al. Surface Doping vs. Bulk Doping of Cathode Materials for Lithium-Ion Batteries: A Review. *Electrochem. Energy Rev.* **2023**, *5*, 2. [[CrossRef](#)]
7. Zhang, N.; Deng, T.; Zhang, S.; Wang, C.; Chen, L.; Wang, C.; Fan, X. Critical Review on Low-Temperature Li-Ion/Metal Batteries. *Adv. Mater.* **2022**, *34*, 2107899. [[CrossRef](#)]
8. Qiu, Q.; Huang, Z. Photodetectors of 2D Materials from Ultraviolet to Terahertz Waves. *Adv. Mater.* **2021**, *33*, e2008126. [[CrossRef](#)] [[PubMed](#)]
9. Feng, C.; Wu, Z.-P.; Huang, K.-W.; Ye, J.; Zhang, H. Surface Modification of 2D Photocatalysts for Solar Energy Conversion. *Adv. Mater.* **2022**, *34*, 2200180. [[CrossRef](#)]
10. Zhu, K.; Zhu, Z.; Jin, B.; Li, H.; Jin, E.; Jeong, S.; Jiang, Q. 3D flower-Like Co_{1-x}S/MoS₂ composite for long-life and high-rate lithium storage. *J. Energy Storage* **2020**, *27*, 101135. [[CrossRef](#)]
11. Olsson, E.; Yu, J.; Zhang, H.; Cheng, H.-M.; Cai, Q. Atomic-Scale Design of Anode Materials for Alkali Metal (Li/Na/K)-Ion Batteries: Progress and Perspectives. *Adv. Energy Mater.* **2022**, *12*, 2200662. [[CrossRef](#)]
12. Ma, W.; Zhang, X.; Meng, Y.; Zhao, J. Hierarchical carbon/MoS₂ composites as anodes for advanced electrochemical performance. *Ionics* **2022**, *28*, 5499–5504. [[CrossRef](#)]
13. Hai, N.Q.; Kim, H.; Yoo, I.S.; Hur, J. Facile and Scalable Preparation of a MoS₂/Carbon Nanotube Nanocomposite Anode for High-Performance Lithium-Ion Batteries: Effects of Carbon Nanotube Content. *J. Nanosci. Nanotechnol.* **2019**, *19*, 1494–1499. [[CrossRef](#)]
14. Kaiyu, Q.; Zeming, Y.; Bangwen, Z. Preparation and electrochemical performance of MoS₂ nanosheets/graphene as anode material. *J. Inn. Mong. Univ. Sci. Technol.* **2019**, *38*, 166–171+176. [[CrossRef](#)]
15. Lee, W.J.; Kim, C.S.; Yang, S.Y.; Lee, D.; Kim, Y.S. Spontaneous Exfoliation of Large-Sized Graphene Oxide with Low Defect Concentration by Simple Wet Chemistry. *Carbon* **2021**, *182*, 214–222. [[CrossRef](#)]
16. Xin, J.; Ying, Z.; Wenhao, H.; Chen, W.; Lili, J.; Lizhi, S. In-Situ Carbon-Coated Molybdenum Disulfide as Anode Material for Lithium-Ion Batteries. *Nonferrous Met. Eng.* **2021**, *11*, 12–16.
17. Jain, R.; Lakhnot, A.S.; Bhimani, K.; Sharma, S.; Mahajani, V.; Panchal, R.A.; Kamble, M.; Han, F.D.; Wang, C.S.; Koratkar, N. Nanostructuring versus microstructuring in battery electrodes. *Nat. Rev. Mater.* **2022**, *7*, 736–746. [[CrossRef](#)]
18. Zhong, Y.; Liu, D.; Wang, L.-T.; Zhu, H.-G.; Hong, G. Controllable synthesis of hierarchical MoS₂ nanotubes with ultra-uniform and superior storage potassium properties. *J. Colloid Interface Sci.* **2020**, *561*, 593–600. [[CrossRef](#)]
19. Choi, W.; Choi, Y.S.; Kim, H.; Yoon, J.; Kwon, Y.; Kim, T.; Ryu, J.-H.; Lee, J.H.; Lee, W.; Huh, J.; et al. Evidence for the Coexistence of Polysulfide and Conversion Reactions in the Lithium Storage Mechanism of MoS₂ Anode Material. *Chem. Mater.* **2021**, *33*, 1935–1945. [[CrossRef](#)]
20. Mateti, S.; Rahman, M.M.; Cizek, P.; Chen, Y. In situ production of a two-dimensional molybdenum disulfide/graphene hybrid nanosheet anode for lithium-ion batteries. *RSC Adv.* **2020**, *10*, 12754–12758. [[CrossRef](#)] [[PubMed](#)]
21. Lee, D.Y.; Seo, S.D.; Song, H.J.; Kim, D.W. Free-standing molybdenum disulfides on porous carbon cloth for lithium-ion battery anodes. *Int. J. Energy Res.* **2021**, *45*, 11329–11337. [[CrossRef](#)]
22. Yu, X.; Tang, J.; Terabe, K.; Sasaki, T.; Gao, R.; Ito, Y.; Nakura, K.; Asano, K.; Suzuki, M.-a. Fabrication of graphene/MoS₂ alternately stacked structure for enhanced lithium storage. *Mater. Chem. Phys.* **2020**, *239*, 121987. [[CrossRef](#)]
23. Ju, W.; Zhu, C.; Wei, Z. Intercalated ion tuning of the cross-plane thermal transport properties of graphite. *AIP Adv.* **2020**, *10*, 095225. [[CrossRef](#)]
24. Fedoseeva, Y.V.; Makarova, A.A.; Stolyarova, S.G.; Arkhipov, V.E.; Ruehl, E.; Okotrub, A.V.; Bulusheva, L.G. Lithium-induced intralayer rearrangement of molybdenum disulfide: Effect of graphene coating. *Appl. Surf. Sci.* **2022**, *598*, 153846. [[CrossRef](#)]
25. Liu, H.; Chen, Y.; Wang, Z.; Zhang, C.; Zhang, X.; Zhou, W.; Liu, J.; Wang, W.; Yu, P. Solid-state reaction synthesis of amorphous/nanostructured Si@SiO₂-Cu₃Si composites by mechanical milling for lithium-ion anodes. *J. Alloys Compd.* **2022**, *905*, 164207. [[CrossRef](#)]
26. Li, X.L.; Li, T.C.; Huang, S.; Zhang, J.; Pam, M.E.; Yang, H. Y Controllable Synthesis of Two-Dimensional Molybdenum Disulfide (MoS₂) for Energy-Storage Applications. *ChemSusChem* **2020**, *13*, 1379–1391. [[CrossRef](#)] [[PubMed](#)]
27. Cao, C.; Dong, H.; Liang, F.; Zhang, Y.; Ge, M. Interfacial Reinforcement Structure Design towards Ultrastable Lithium Storage in MoS₂-based Compositing Electrode. *Chem. Eng. J.* **2021**, *416*, 129094. [[CrossRef](#)]
28. Wei, X.; Lin, C.-C.; Wu, C.; Qaiser, N.; Cai, Y.; Lu, A.-Y.; Qi, K.; Fu, J.-H.; Chiang, Y.-H.; Yang, Z.; et al. Three-dimensional hierarchically porous MoS₂ foam as high-rate and stable lithium-ion battery anode. *Nat. Commun.* **2022**, *13*, 6006. [[CrossRef](#)] [[PubMed](#)]
29. Zhao, Z.; Shen, S.; Chen, F.; Zhong, M.; Chew, J.W. Preparation and Properties of Mesoporous Carbon Composite as Negative Electrode Materials. *Int. J. Electrochem. Sci.* **2019**, *14*, 10058–10069. [[CrossRef](#)]
30. Volkov, A.I.; Eliseeva, S.N.; Tolstopjatova, E.G.; Kondratiev, V.V. Enhanced electrochemical performance of MoS₂ anode material with novel composite binder. *J. Solid State Electrochem.* **2020**, *24*, 1607–1614. [[CrossRef](#)]

31. Zhong, W.; Hong, J.; Wang, C.; Li, Z.; Chen, J.; Dmytro, S. MoS₂/graphene nanosheet composites prepared by xylitol-assisted ball milling as high-performance anode materials for lithium-ion batteries. *Ionics* **2022**, *29*, 917–930. [[CrossRef](#)]
32. Zhang, L.; Chen, C. Electrode Materials for Lithium Ion Battery. *Prog. Chem.* **2011**, *23*, 275–283.
33. Lee, Y.K. Effect of transition metal ions on solid electrolyte interphase layer on the graphite electrode in lithium ion battery. *J. Power Sources* **2021**, *484*, 229270. [[CrossRef](#)]
34. Jha, V.; Krishnamurthy, B. Modeling the SEI layer formation and its growth in lithium-ion batteries (LiB) during charge-discharge cycling. *Ionics* **2022**, *28*, 3661–3670. [[CrossRef](#)]
35. Marriam, I.; Tebyetekerwa, M.; Chen, H.; Chathuranga, H.; Motta, N.; Alarco, J.A.; He, Z.-J.; Zheng, J.-C.; Du, A.; Yan, C. Few-layer MoS₂ nanosheets with and without silicon nanoparticles as anodes for lithium-ion batteries. *J. Mater. Chem. A* **2023**, *11*, 2670–2678. [[CrossRef](#)]
36. Li, R.; O’Kane, S.; Marinescu, M.; Offer, G.J. Modelling Solvent Consumption from SEI Layer Growth in Lithium-Ion Batteries. *J. Electrochem. Soc.* **2022**, *169*, 060516. [[CrossRef](#)]
37. Heidrich, B.; Boerner, M.; Winter, M.; Niehoff, P. Quantitative determination of solid electrolyte interphase and cathode electrolyte interphase homogeneity in multi-layer lithium ion cells. *J. Energy Storage* **2021**, *44*, 103208. [[CrossRef](#)]
38. Nguyen, Q.H.; Hur, J. MoS₂-TiC-C Nanocomposites as New Anode Materials for High-Performance Lithium-Ion Batteries. *J. Nanosci. Nanotechnol.* **2019**, *19*, 996–1000. [[CrossRef](#)] [[PubMed](#)]
39. Li, Z.; Ottmann, A.; Thauer, E.; Neef, C.; Sai, H.; Sun, Q.; Cendrowski, K.; Meyer, H.P.; Vaynzof, Y.; Mijowski, E. A facile synthesis method and electrochemical studies of hierarchical structured MoS₂/C-nanocomposite. *arXiv* **2017**, arXiv:1701.05894. [[CrossRef](#)]
40. Cong, R.; Park, H.-H.; Jo, M.; Lee, H.; Lee, C.-S. Synthesis and Electrochemical Performance of Electrostatic Self-Assembled Nano-Silicon@N-Doped Reduced Graphene Oxide/Carbon Nanofibers Composite as Anode Material for Lithium-Ion Batteries. *Molecules* **2021**, *26*, 4831. [[CrossRef](#)]
41. Liu, Y.; Zhang, C.; Cui, J.; Wei, W. Graphene enwrapped molybdenum disulfide for long life rechargeable batteries. *Mater. Express* **2020**, *10*, 1358–1363. [[CrossRef](#)]
42. Lee, S.; Kwon, S.; Kim, K.; Kang, H.; Ko, J.M.; Choi, W. Preparation of Carbon Nanowall and Carbon Nanotube for Anode Material of Lithium-Ion Battery. *Molecules* **2021**, *26*, 6950. [[CrossRef](#)] [[PubMed](#)]
43. Hou, S.X.; Wu, C.; Huo, Y.J. Controllable Preparation of Nano Molybdenum Disulfide by Hydrothermal Method. *Ceram.-Silik.* **2017**, *61*, 158–162. [[CrossRef](#)]
44. Shelke, N.T.; Karle, S.C.; Karche, B.R. Hydrothermal Growth and Humidity-Dependent Electrical Properties of Molybdenum Disulfide Nanosheets. *J. Nanosci. Nanotechnol.* **2019**, *19*, 5158–5166. [[CrossRef](#)]
45. Ma, L.; Zhou, X.; Xu, L.; Xu, X.; Zhang, L. Microwave-Assisted Hydrothermal Preparation of SnO₂/MoS₂ Composites and their Electrochemical Performance. *Nano* **2016**, *11*, 1650023. [[CrossRef](#)]
46. Zhai, Y.-J.; Li, J.-H.; Chu, X.-Y.; Xu, M.-Z.; Li, X.; Fang, X.; Wei, Z.-P.; Wang, X.-H. Preparation and Application of Molybdenum Disulfide Nanostructures. *J. Inorg. Mater.* **2015**, *30*, 897–905.
47. Zhao, Z.; Shen, S.; Li, Y.; Chen, Q.; Yu, X.; Zhong, M.; Chen, X. Preparation and Electrochemical Properties of bowl-shaped carbon/molybdenum disulfide composite as cathode material for Lithium Ion Batteries. *Int. J. Electrochem. Sci.* **2020**, *15*, 6290–6301. [[CrossRef](#)]
48. Takahashi, Y.; Nakayasu, Y.; Iwase, K.; Kobayashi, H.; Honma, I. Supercritical hydrothermal synthesis of MoS₂ nanosheets with controllable layer number and phase structure. *Dalton Trans.* **2020**, *49*, 9377–9384. [[CrossRef](#)] [[PubMed](#)]
49. Jiang, X.; Chen, Y.; Meng, X.; Cao, W.; Liu, C.; Huang, Q.; Naik, N.; Murugadoss, V.; Huang, M.; Guo, Z. The impact of electrode with carbon materials on safety performance of lithium-ion batteries: A review. *Carbon* **2022**, *191*, 448–470. [[CrossRef](#)]
50. Zhao, L.; Ding, B.; Qin, X.-Y.; Wang, Z.; Lv, W.; He, Y.-B.; Yang, Q.-H.; Kang, F. Revisiting the Roles of Natural Graphite in Ongoing Lithium-Ion Batteries. *Adv. Mater.* **2022**, *34*, 2106704. [[CrossRef](#)]
51. Tan, J.; Tan, X.; Kang, W.; Zhang, C. Two Dimensional Molybdenum Disulfide/Graphite Composites Prepared by Direct All-Solid-State Ball-Milling for Lithium-Ion Batteries. *Chin. J. Appl. Chem.* **2017**, *34*, 810–817.
52. Wang, M.; Dang, D.Y.; Meyer, A.; Arsenaault, R.; Cheng, Y.T. Effects of the Mixing Sequence on Making Lithium Ion Battery Electrodes. *J. Electrochem. Soc.* **2020**, *167*, 100518. [[CrossRef](#)]
53. Wang, Z.; Wei, G.; Ozawa, K.; Cai, Y.; Cheng, Z.; Kimura, H. Nanoporous MoS₂/C Composites for High Performance Lithium Ion Battery Anode Material. *Electrochim. Acta* **2017**, *239*, 74–83. [[CrossRef](#)]
54. Murray, V.; Hall, D.S.; Dahn, J.R. A Guide to Full Coin Cell Making for Academic Researchers. *J. Electrochem. Soc.* **2019**, *166*, A329–A333. [[CrossRef](#)]

Disclaimer/Publisher’s Note: The statements, opinions and data contained in all publications are solely those of the individual author(s) and contributor(s) and not of MDPI and/or the editor(s). MDPI and/or the editor(s) disclaim responsibility for any injury to people or property resulting from any ideas, methods, instructions or products referred to in the content.